Photoionization of the $5d6p\ ^3D_1$ state of barium

Darrell J. Armstrong, Robert P. Wood, and Chris H. Greene
Joint Institute for Laboratory Astrophysics of the University of Colorado and National Institute of Standards and Technology, and Department of Physics, University of Colorado, Boulder, Colorado 80309-0440
(Received 29 October 1992)

We have carried out a relative measurement of the photoionization cross section of the $5d6p\ ^3D_1$ state of barium from the $6s$ ionization threshold to 875 cm^{-1} ($\sim$0.109 eV) above the $5d_{5/2}$ ionization threshold. The cross section was measured for two different final-state symmetries by varying the angle between the laser polarization vectors. Both photoionization cross sections contain "forbidden lines" which arise through a breakdown of the selection rules on J and M_J due to the hyperfine interaction in the odd isotopes of barium. These experimental results are compared with jj-coupled eigenchannel R-matrix calculations and show good agreement. Approximate incorporation of the hyperfine effects into the calculations was necessary for a complete understanding of the measured photoionization cross sections. We found that for the odd isotopes ($\sim$18% of natural barium) the excited $5d6p\ ^3D_1$ state was substantially depolarized by the effect of the hyperfine interaction.

PACS number(s): 32.80.Fb, 32.80.Rm, 32.80.Dz

INTRODUCTION

Photoionization cross sections of the alkaline-earth atoms have received considerable attention both experimentally and theoretically. In particular, photoionization of the low-lying $6s6p\ ^1P_1$ excited state of barium has been somewhat controversial. Until recently, agreement between different theoretical approaches [1–3], as well as agreement between theory and both absolute [4–7] and strictly relative [8,9] photoionization cross-section measurements was unsatisfactory. Generally good agreement has now been achieved between the relative measurement of the $6s6p\ ^1P_1$ cross section of Ref. [8] and a *nearly ab initio* jj-coupled eigenchannel R-matrix calculation in combination with multichannel quantum defect theory (MQDT) [10]. (Here *nearly ab initio* implies that some experimentally derived quantities, in this case ionization threshold values, are used in the calculation.) With these recent results the eigenchannel R-matrix plus MQDT method has now been shown to give good agreement when applied to ground-state, low-lying excited state, and highly excited Rydberg state photoionization in the alkaline-earth elements [3 and references therein].

A central point of the theoretical treatment of Ref. [10] was the inclusion of hyperfine effects in the odd isotopes of natural barium (^{135,137}Ba) to explain the presence of certain unexpected features in the photoionization spectrum of Ref. [8]. These "forbidden" features arise in experimental measurements of photionization cross sections when the hyperfine structure in an excited state (if present) leads to a breakdown of the selection rules on J and M_J that depend on the angle between laser polarization vectors. The breakdown of these selection rules in excited state photoionization of the alkaline-earth atom barium can lead to somewhat striking unexpected resonances that do not belong to the final-state symmetry selected by a given experiment. Although the calculations performed in Ref. [10] successfully reproduced the $6s6p\ ^1P_1$ photoionization cross section measured in Ref. [8], including the forbidden resonances, a measurement of a different excited state cross section would provide another test of the validity of the methods of Ref. [10]. With this purpose in mind, we have carried out a relative measurement of the photoionization cross section of the $5d6p\ ^3D_1$ state of barium. This more diffuse and slightly higher-lying doubly excited state differs qualitatively in the nature of its wave function from the singly excited $6s6p\ ^1P_1$ state studied previously. This measurement serves to test the validity of the interpretation of Wood, Greene, and Armstrong in Ref. [10], and it provides a further test of the eigenchannel R-matrix method for calculating excited state photoionization cross sections.

In the past, some portions of this photoionization cross section have been measured using experimental techniques similar to those described in this work [11]. In addition, optogalvanic spectra of the even-parity levels above the Ba+6s threshold have been recorded from the $5d6p\ ^3P_{1,2}$, $^3F_{3,4}$, and $^1P_1$ excited states with accurate wavelength calibration [12]. (Many of the autoionizing resonances in the cross sections presented here are classified in Ref. [12], and in an MQDT analysis of the Ba even-parity spectrum below the $5d_{3/2}$ threshold [13].) However, a measurement that recorded the entire barium $5d6p\ ^3D_1$ photoionization cross section from the $6s$ threshold to beyond the $5d_{5/2}$ threshold has not, to the authors' knowledge, been presented before. Thus this work provides a measurement which, within experimental constraints, faithfully represents the locations, line shapes, and intensities of the many interacting channels converging to their respective ionization thresholds. Such a measurement is necessary for a comprehensive test of theory.

EXPERIMENT

The experimental photoionization cross sections presented here were measured with two pulsed dye lasers

of the Littman configuration which excited and ionized barium atoms in a thermal atomic beam. Both lasers were pumped by the third harmonic of a neodymium-doped yttrium aluminum garnet (Nd:YAG) laser at a 10 Hz repetition rate and had linewidths of ~ 05 cm^{-1} and pulse duration of 5 ns. The first laser was tuned into resonance with the transition from the $6s^2\,{}^1S_0$ ground state to the $5d6p\,{}^3D_1$ state at a vacuum wavelength of 413.4 nm. The second (scanning) laser was tuned continuously between 561 and 410 nm to cover the energy range from the Ba+6s threshold to 875 cm^{-1} above the Ba+$5d_{5/2}$ threshold. To reduce unwanted photoionization by the first laser of any bound states excited by the scanning laser, the second laser pulse was delayed by 8 ns with respect to the first. The 8 ns delay was a good precautionary measure, but the only bound state other than the $5d6p\,{}^3D_1$ with $J=1$ and odd parity in the entire energy range of this experiment was the $6s6p\,{}^1P_1$ level. To provide good overlap between the individual data sets in this energy range, eight different dyes were used in the scanning laser.

At the point of intersection with the atomic beam, both lasers were focused to spot sizes of approximately 0.02 cm^2. The pulse energy of the first laser was adjusted to ~ 2 μJ which minimized direct photoionization of the $5d6p\,{}^3D_1$ state by a second 413.4 nm photon and yet provided an adequate excited state population. The pulse energy of the second laser was set to a maximum of 40 μJ at the peak of the efficiency curve for each dye. This pulse energy resulted in minimal apparent broadening of the autoionizing resonances due to depletion of the excited $5d6p\,{}^3D_1$ state. The effect of depletion broadening [14] as a function of laser pulse energy was investigated for the $5d_{5/2}7d_{5/2}$ $J=0$ state just above the 6s threshold at ~ 550 nm. For this experimental setup, broadening became significant for a pulse energy of approximately 80 μJ, where the full width at half maximum (FWHM) of the $5d_{5/2}7d_{5/2}$ $J=0$ state was roughly 30% greater than the FWHM measured at lower pulse energies. Increases in width for this state were only a few percent over a lower range of pulse energies from 10 to 40 μJ. This test was not repeated elsewhere in the cross section where the autoionizing resonances are much narrower. Since we observed a few percent depletion broadening for a naturally broad resonance near the 6s threshold, it follows that the narrower resonances were also broadened by some small amount over that due to the 0.5 cm^{-1} laser linewidth. With the observed depletion broadening as a guide to set the scanning laser pulse energy, the barium ion signal was reliably proportional to the laser intensity over the entire effective scan range of each dye used in this experiment.

The nearly collinear laser beams intersected the atomic beam between two field plates separated by 1 cm in a vacuum chamber with a background pressure of $\sim 2\times 10^{-7}$ torr. The atom density at the intersection point was estimated to be $\leq 10^9$ cm^{-3}. Data were collected only after the atomic beam oven temperature had stabilized to $\sim 600\,^\circ$C to assure constant beam density. Barium ions were collected in an electron multiplier by applying a 20 V pulse to the field plate farthest from the multiplier 3 μs after the lasers fired. The field plate nearest to the electron multiplier had a 1 mm wide slit in its center which was covered with fine electroformed mesh for the ions to pass through. This field plate was held at ground potential at all times, while the other plate was held at a quiescent voltage of ≤ 2 mV during excitation due to the pulse electronics. Any other sources of stray electric fields were carefully shielded, and all static magnetic fields at the interaction region were nulled with Helmholtz coils external to the vacuum chamber. The ion signal was sent to a gated integrator and boxcar averager. The signal from the averager, along with the scanning laser intensity and an étalon fringe signal were all recorded at 1 s intervals in a computer-based data-acquisition system. For the entire experiment the interval between data points, measured in scanning laser frequency, was about 4.5 GHz.

The wavelength of the scanning laser was measured at the beginning of each data run by a monochromator with absolute calibration of ± 0.05 nm. The wavelength at all other data points was determined relative to the first data point from the fringe signal of an étalon with a 101 GHz free spectral range. When the data were analyzed, the experimental air wavelengths were converted to vacuum wavelengths. Wavelength calibration was then verified by comparing the location of the measured resonances against known values for the even-parity levels of barium above the 6s threshold [12,13], and by using the increase in photoionization signal when the scanning laser came into resonance with the excited $5d6p\,{}^3D_1$ state at 413.4 nm near the end of the measured spectrum. Small corrections in the absolute wavelength were made if necessary to correct for the uncertainty in the monochromator calibration. Using this procedure, we found the largest estimated error in wavelength for any portion of this photoionization spectrum was on the order of 0.2 nm.

The intensity of the scanning laser was monitored with a photodiode which had an output signal that was linear for the laser intensities used in this experiment. After wavelengths were assigned to the data points, the recorded scanning laser intensity signal was corrected for the spectral response of the photodiode. The ion signal was then normalized with respect to the corrected scanning laser intensity. This procedure is strictly valid only when there is no saturation of the ion signal since normalization to laser intensity cannot correct for the effects of depletion broadening. To facilitate connecting the data for all eight dyes into one complete photoionization spectrum, all parameters that affect ion signal size were held constant throughout this experiment. The separate portions of the photoionization spectrum obtained with the different dyes were then easily joined by comparing baseline values and the heights of resonances common to individual scans that overlapped in wavelength.

Two complete measurements of the photoionization spectrum were made for two different final-state symmetries. For two-step resonant excitation with both lasers linearly polarized, selection rules that depend on the angle between polarization vectors resulted in $M_J=0$, $J=0$ or 2 for parallel polarization, or $|M_J|=1$, $J=1$ or 2

for perpendicular polarization. Here the quantization axis was chosen to lie along the polarization vector of the first laser. The two laser beams were verified to have parallel linear polarization by adjusting the linear polarizer for each laser while monitoring extinction of the laser light that passed through a third polarizer oriented perpendicular to both of the laser polarizers. The parallel orientation of the polarizers was then used as a reference to rotate the scanning laser polarizer 90° for the perpendicular polarization measurement. Great care was taken when setting the orientation of the polarizers before each data run. Any forbidden features in the cross section could then be reliably attributed to the hyperfine interaction or any other possible cause not associated with the laser polarization.

THEORY

The photoionization cross section of the $5d6p\ ^3D_1$ state of barium was calculated using the eigenchannel R-matrix approach in combination with multichannel quantum defect theory which is described in detail elsewhere [3]. The entire calculation was performed in jj coupling with the spin-orbit interaction included explicitly within the R-matrix box. An R-matrix box size of $r_0=22$ a.u. was found to be sufficient to contain the $5d6p\ ^3D_1$ wave function. All calculations presented here were convolved with a Gaussian line profile of 0.5 cm^{-1} FWHM to account for the bandwidth of the ionizing laser.

It was shown in Ref. [10] that the cross section for photoionization of a $J=1$ state that was excited from a $J=0$ ground state in which both the exciting and photoionizing lasers are linearly polarized has the general form

$$\begin{aligned}\sigma_{\rm lin}(J_0\rightarrow J_e\rightarrow J_f)=&\sigma^{(\rm iso)}(1\rightarrow 0)\{1+2g_{\rm av}^{(2)}P_2(\cos\theta)\}\\&+\sigma^{(\rm iso)}(1\rightarrow 1)\{1-g_{\rm av}^{(2)}P_2(\cos\theta)\}\\&+\sigma^{(\rm iso)}(1\rightarrow 2)\{1+\tfrac{1}{5}g_{\rm av}^{(2)}P_2(\cos\theta)\}\ .\end{aligned}\tag{1}$$

In this expression, θ is the angle between the linear polarization vectors of the exciting and photoionizing lasers, and $P_2(\cos\theta)$ is a Legendre polynomial. $\sigma^{(\rm iso)}(J_e\rightarrow J_f)$ is the "isotropic" cross section for photoionization of the excited state and is given in a.u. by

$$\sigma_{(\rm iso)}(J_e\rightarrow J_f)=\frac{4\pi^2\alpha\omega}{3(2J_e+1)}|\langle J_f\|r^{(1)}\|J_e\rangle|^2\ ,\tag{2}$$

where $\langle J_f\|r^{(1)}\|J_e\rangle$ is a reduced matrix element, ω is the angular frequency of the second (ionizing) photon, and α is the fine-structure constant. "Isotropic" in this context means that $\sigma^{(\rm iso)}(J_e\rightarrow J_f)$ is the total photoionization cross section for the channel $J_e\rightarrow J_f$ which would be calculated if the excited state $|J_e\rangle$ were randomly oriented, i.e., with equal population in all of the magnetic sublevels M_{J_e}. The factor $g_{\rm av}^{(2)}$ in Eq. (1) contains the effects of the hyperfine interaction on the excited state and represents an average over time and over relative isotopic abundances. Specifically, $g_{\rm av}^{(2)}$ represents the average of an expression for the time dependence of the quadrupole moment caused by the hyperfine interaction in the excited state. This time-dependent factor is given by [10]

$$g^{(2)}(t)=\sum_{F,F'}\frac{(2F+1)(2F'+1)}{(2I+1)}\cos(\omega_{FF'}t)\times\begin{Bmatrix}F & F' & 2\\ J_e & J_e & I\end{Bmatrix}^2\ .\tag{3}$$

In this expression, I is the nuclear spin, $\mathbf{F}=\mathbf{I}+\mathbf{J}$ is the total angular momentum, t is the delay between two laser pulses, and $\omega_{FF'}$ derives from the hyperfine splitting of different F levels in the excited state. In the derivation of Eq. (3), both lasers have been assumed to have a pulse duration τ much shorter than all hyperfine precession periods, i.e., $\tau\ll 2\pi\omega_{FF'}^{-1}$. Consequently, the applicability of Eq. (3) to experiments such as this one is far from obvious as the measurements were made with $\tau\approx 2\pi\omega_{FF'}^{-1}$ by multimode pulsed dye lasers with pulses that exhibited significant mode beating. The pulse durations were approximately $\tau\sim 5$ ns, while the hyperfine splittings for the excited ^{137}Ba $5d6p\ ^3D_1$ state have been measured [15] to be $\omega_{5/2,1/2}/2\pi=605$ MHz, $\omega_{5/2,3/2}/2\pi=428$ MHz, and $\omega_{3/2,1/2}/2\pi=177$ MHz. Despite the fact that the inequality $\tau\ll 2\pi\omega_{FF'}^{-1}$ is not accurately satisfied, we assume that the hyperfine precession effects can still be described qualitatively by averaging $g^{(2)}(t)$ over time and over barium isotopic abundances to give an effective depolarization $g_{\rm av}^{(2)}$.

While the time-averaged $g_{\rm av}^{(2)}$ is appropriate for this work, $g^{(2)}(t)$ in Eq. (3) can be examined to establish two important physical limits for the effect of the hyperfine interaction. In the limit that $\omega_{FF'}t\ll 1$ (δ-function pulses, time delay ≈ 0), $g^{(k)}(t)\approx 1$ and the excited state is completely polarized because the hyperfine effect plays no role (i.e., in the vector model picture, there is no time for precession of $\mathbf{J}$ about the total angular momentum $\mathbf{F}$). In the opposite limit where $\omega_{FF'}t\gg 1$, all terms in Eq. (3) with $F\neq F'$ effectively average to zero and can be neglected. This will be referred to as the limit of complete depolarization. When the relative isotopic abundances of natural barium are taken into account ($\sim 18\%$ have $I=3/2$), a limit of complete depolarization for $g_{\rm av}^{(2)}$ can be established to be

$$g_{\rm av}^{(2)}=0.864\ .$$

Since a value of $g_{\rm av}^{(2)}\approx 1$ would imply that there is no depolarization of the excited state, a physical result for $g_{\rm av}^{(2)}$ for photoionization in natural barium, where the condition $\tau\geq 2\pi\omega_{FF'}^{-1}$ applies, is expected to lie between 0.864 and 1.

RESULTS AND DISCUSSION

The experimental Ba $5d6p\ ^3D_1$ state photoionization cross sections for both final-state symmetries, for the entire region from the $6s$ threshold to beyond the $5d_{5/2}$ threshold, are plotted against the vacuum wavelength of the ionizing laser in Figs. 1(a) and 2(a). (Although the experimental measurements included the $6s$ threshold at ~ 560.4 nm, there is no structure of interest beyond 560 nm). Figures 3(a) and 4(a) provide a much closer look at the photoionization cross sections in Figs. 1(a) and 2(a)

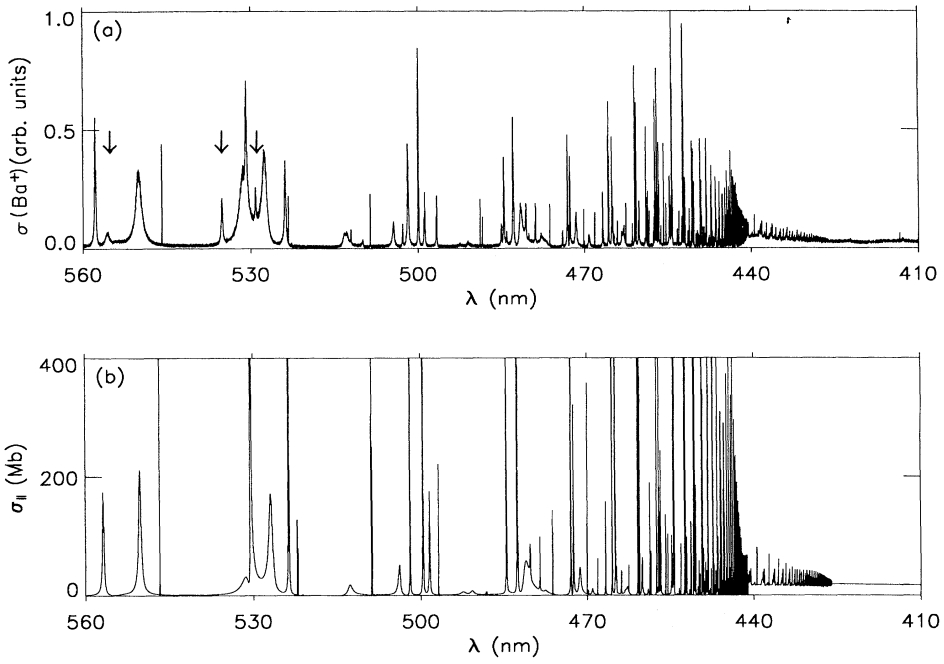

FIG. 1. (a) Relative experimental photoionization cross section vs ionizing laser wavelength for the Ba $5d6p\ ^3D_1$ state for parallel polarization ($M_J=0$, $J=0,2$) from the $6s$ threshold to 875 cm^{-1} above the $5d_{5/2}$ threshold. Arrows denote forbidden $|M_J|=1$ resonances. (b) Calculated photoionization cross section for the same final-state symmetry and energy range as in (a), ignoring hyperfine depolarization effects.

for the region between 444 and 424 nm, which includes the $5d_{3/2}$ threshold at 440.2 nm and the $5d_{5/2}$ threshold at 425.2 nm. In the region below the $5d_{3/2}$ threshold in Figs. 1(a) and 2(a) we see the irregular spacing of autoionizing resonances indicative of the many interacting channels converging to the two different thresholds. The line profiles in this energy range are predominantly symmetric (high Fano q parameter). Note how the familiar window resonances ($q\approx 0$) found in photoionization of the ground state or of the $6s6p\ ^1P_1$ state are absent, since direct excitation to the structureless $6s$ continuum from the $5d6p\ ^3D_1$ state is quite weak. Also nearly absent in the parallel polarization measurement is the broad $6p^2\ ^1S_0$ autoionizing complex that is such a striking feature in the $6s6p\ ^1P_1$ photoionization cross section [1,3,8,16]. This feature, which appears as a very broad but weak structure in the midst of narrower resonances, lies roughly between 475 and 485 nm in Fig. 1(a). Although the $6p^2\ ^1S_0$ state has even parity, its dipole matrix element to the excited $5d6p\ ^3D_1$ state is evidently very small, as expected in LS coupling. In the energy range between the $5d_{3/2}$ threshold and the $5d_{5/2}$ threshold in

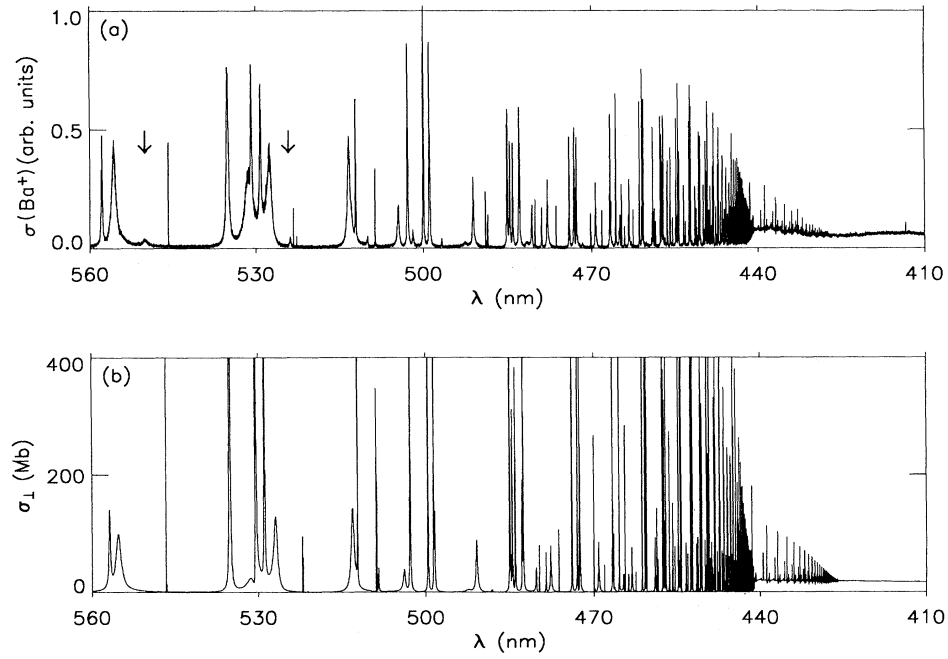

FIG. 2. (a) Relative experimental photoionization cross section vs ionizing laser wavelength for the Ba $5d6p\ ^3D_1$ state for perpendicular polarization ($|M_J|=1$, $J=1,2$) from the $6s^+$ threshold to 875 cm^{-1} above the $5d_{5/2}$ threshold. Arrows denote forbidden $M_J=0$ resonances. (b) Calculated photoionization cross section for the same final-state symmetry and energy range as in (a), ignoring hyperfine depolarization effects.

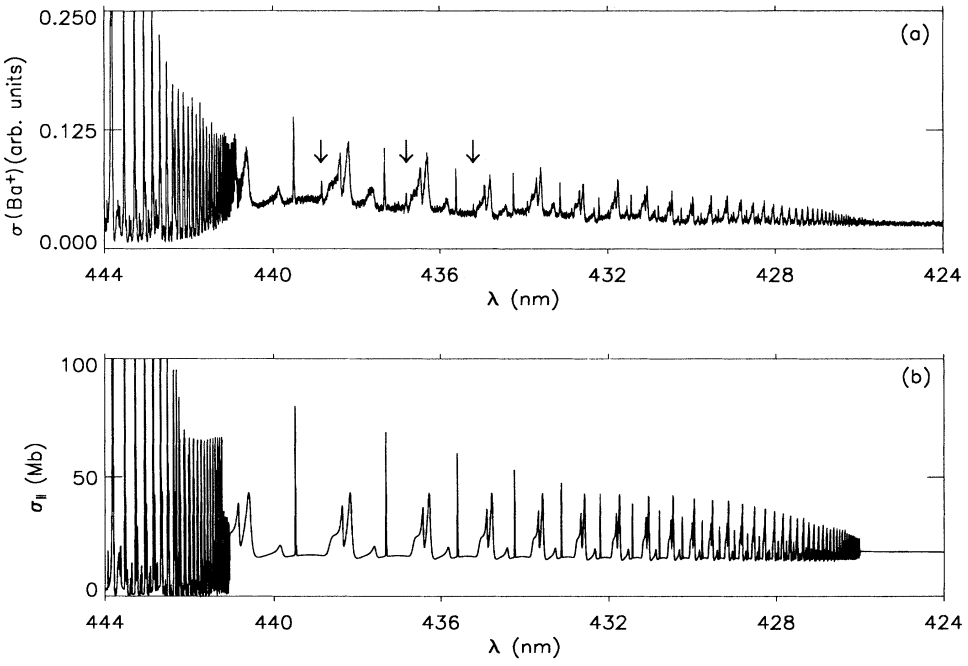

FIG. 3. (a) The parallel polarization cross section as in Fig. 1(a), but only for the narrow energy range near the $5d_{3/2}$ and $5d_{5/2}$ thresholds. Arrows denote forbidden $|M_J|=1$ resonances. (b) Calculated photoionization cross section for the same final-state symmetry and energy range as in (a).

Figs. 3(a) and 4(a), there is now direct excitation to the $5d_{3/2}$ continuum and there are only the various Rydberg channels converging to the higher-lying $5d_{5/2}$ threshold. We can identify several regularly spaced series of states with asymmetric profiles, especially for the $J=1$ resonances in the perpendicular polarization measurement of Fig. 4(a). [The oscillation of the base line in Fig. 4(a) near 428 nm is an experimental artifact that pertains to the scanning laser.] Above the $5d_{5/2}$ threshold there is only a structureless continuum in the energy range covered here, except for the increase in direct photoionization of the $5d6p\ ^3D_1$ state seen in Figs. 1(a) and 2(a) when the scanning laser passes through 413.4 nm. The slightly elevated base lines below the $5d_{3/2}$ threshold in the experimental measurements (as compared to the calculated cross sections) are present because of the small but constant photoionization of the $5d6p\ ^3D_1$ state by a second photon from the first laser into the continuum above the $5d_{5/2}$ threshold.

In all four of the experimental cross sections shown in Figs. 1(a), 2(a), 3(a), and 4(a), arrows denote just a few of the easily identified forbidden lines due to the hyperfine

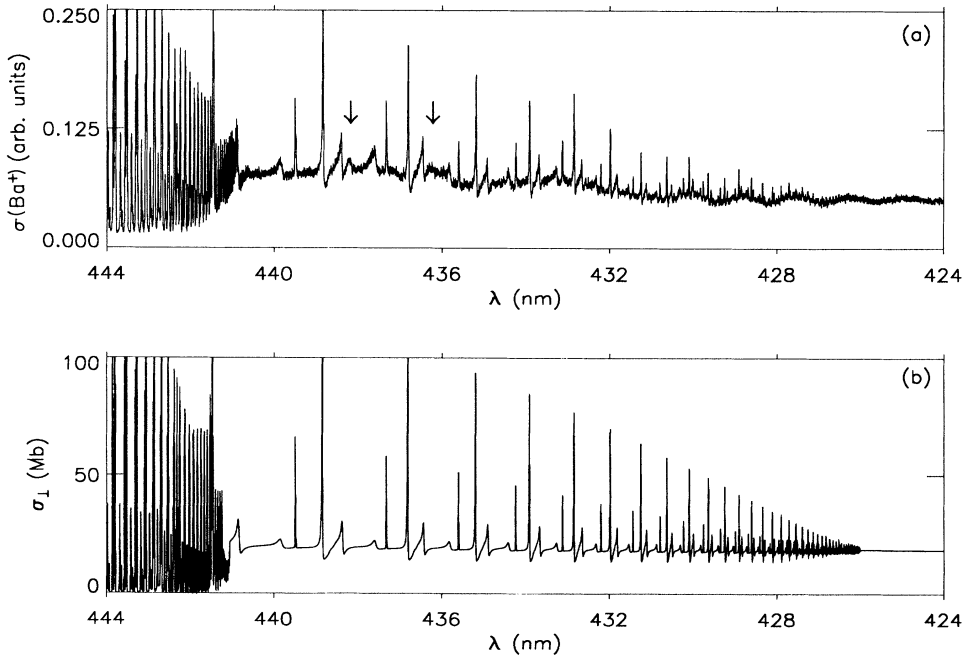

FIG. 4. (a) The perpendicular polarization cross section as in Fig. 2(a), but only for the narrow energy range including the $5d_{3/2}$ and $5d_{5/2}$ thresholds. Arrows denote forbidden $M_J=0$ resonances. (b) Calculated photoionization cross section for the same final-state symmetry and energy range as in (a).

interaction. In Figs. 1(a) and 2(a), the region just above the $6s$ threshold contains conspicuous forbidden features easily identified due to the low density of states. In Fig. 3(a) we can see a series of narrow forbidden lines above the $5d_{3/2}$ threshold due to the strong asymmetric $J=1$ resonance in the perpendicular polarization measurement of Fig. 4(a). In Fig. 4(a) there is a much less conspicuous but nonetheless identifiable series of broad forbidden resonances above the $5d_{3/2}$ threshold due to the $J=0$ resonances in the parallel polarization measurement of Fig. 3(a). It is easy to identify these features since the *forbidden* lines present have angular momentum labels $M_J=0$, $J=0$ and $|M_J|=1$, $J=1$, respectively, in the parallel and perpendicular polarization measurements. Barring an accidental coincidence of a $J=0$ and $J=1$ resonance, any feature common to both measurements must have $J=2$. As is evident in Figs. 1(a) and 2(a), the forbidden lines in these photoionization cross sections are quite prominent. These strong forbidden features indicate that understanding the breakdown of the polarization-dependent selection rules on J and M_J is in general essential to interpreting photoionization processes in natural barium. It should be mentioned that a unique exception to this statement exists when the linear polarizers for the exciting and photoionizing lasers are adjusted so that θ in Eq. (1) is set to the "magic" angle of 54.7° where $P_2(\cos\theta)=0$. For this angle only, hyperfine depolarization of the excited state has no effect on the photoionization cross section, as shown in Refs. [4,10].

The corresponding theoretical photoionization cross sections for both final-state symmetries are shown below the respective experimental results in Figs. 1(b), 2(b), 3(b), and 4(b). The entire calculated cross sections as shown in Figs. 1(b) and 2(b) each contain approximately 94 000 total energy mesh points prior to convolution with the laser linewidth. For the range of wavelengths greater than 460 nm, where the density of states is relatively low, the cross section was calculated with only 8700 mesh points equally spaced in energy. For wavelengths shorter than 460 nm, where both $5d$ thresholds are located and the density of states is much greater, the cross section was calculated with approximately 85 000 mesh points which are nonuniformly spaced in energy and concentrated at the resonances. In this wavelength range, a typical 90 000 point calculation between 460 and 420 nm for the 14 channel $J=2$ final-state symmetry required 50 min of CPU time on a DEC station 5240. Clearly, this example calculation demonstrates the efficiency of the eigenchannel R-matrix plus MQDT method for reproducing complicated photoionization cross sections.

As discussed earlier, the calculated cross sections in Figs. 1(b), 2(b), 3(b), and 4(b) have been convolved with a laser linewidth of 0.5 cm^{-1} to help achieve better agreement with the experimental results. However, none of these calculated cross sections includes the correction for hyperfine effects given by Eqs. (1)–(3). Aside from the obvious absence of forbidden lines, agreement between the theoretical cross sections and the experimental results is generally quite good. For the very broad resonances near the $6s$ threshold, and for the various Rydberg series converging to the $5d_{5/2}$ threshold, the line shapes for the experiment and theory probably show the best agreement. One exception to the good agreement for the resonances found near the $6s$ threshold is the broad shoulder on the long-wavelength side of the $5d_{3/2}8d$ $J=2$ resonance at 530.8 nm. The calculation apparently underestimates the height of this shoulder as seen by comparing the theoretical cross section in Fig. 1(b) and 2(b) with the experimental measurement of Figs. 1(a) and 2(a). The calculation also includes a pronounced asymmetric dip in the cross section between the shoulder and the taller, narrower $J=2$ resonance. Although agreement between theory and experiment is generally good for the broader resonances between the $6s$ and $5d_{3/2}$ thresholds, many of the narrower peak heights for this energy range are substantially higher in the theoretical results of Figs. 1(b), 2(b), 3(b), and 4(b). (These theoretical peak heights reach as high as 45 052 and 33 789 Mb, respectively, in the parallel and perpendicular cross sections. We have plotted the calculated cross sections up to only 400 Mb in Figs. 1 and 2, and up to only 100 Mb in Figs. 3 and 4. If the calculated cross sections were not cut off at these values, comparison with the measurements would be difficult, if not impossible for the weaker features in the cross sections.) One contribution to these discrepancies may be the effect of the small amount of depletion broadening discussed earlier in the section on experimental details. It is also entirely possible that despite convolution with the laser linewidth of 0.5 cm^{-1}, the calculations overestimate the heights of the narrow resonances. It is unlikely that an experiment such as this one performed with broad-bandwidth multimode pulsed lasers is capable of resolving these discrepancies.

Another area where theory and experiment show inconsistent agreement is the location of resonances throughout various regions of the photoionization spectrum. In the region above the $5d_{3/2}$ threshold in Figs. 3(a) and 3(b) as well as in Figs. 4(a) and 4(b), the locations of the various channels converging to the $5d_{5/2}$ threshold show very good agreement. Part of the reason that these resonances lined up so well was the inclusion of well-known experimentally derived values for the ionization thresholds in the eigenchannel R-matrix calculation. The $5d$ thresholds themselves are of course difficult to locate in the experimental results since finite laser bandwidth led to a measured photoionization cross section which was continuous across these thresholds. The $5d$ thresholds are also difficult to exactly locate in the theoretical results since the continuous behavior of the photoionization cross sections near threshold was included in the calculations by performing a "Gailitis average" [17]. This amounts to an average over resonances just below a threshold, and it is easily accomplished in an MQDT calculation by treating the most weakly closed channels as if they were open when solving the MQDT equations. The resulting calculated cross sections are continuous across the thresholds, in fairly good agreement with the experimental results. On an energy scale, poorer agreement between experimental and theoretical resonance positions is found in other regions of the spectrum, especially between 560 and 500 nm in Figs. 1(a) and 1(b) and in Figs. 2(a) and 2(b). Two conspicuous examples are the group

of resonances near 500 nm and the narrow $5d_{3/2}5g_{7/2}$ $J=2$ resonances at 545.9 nm just above the 6s threshold. The experimental locations in Figs. 1(a) and 2(a) agreed quite well with the results of earlier optogalvanic measurements [13] even before adjustments for the monochromator calibration were made. The consistency of the two experimental results suggests that the calculated locations of resonances below the $5d_{3/2}$ threshold have room for improvement. A comparison of the experimental and theoretical energy values for the $5d_{3/2}5g_{7/2}$ $J=2$ resonance reveals that the calculated g-channel quantum defect at this energy is too large by approximately 0.0158. This is in the range of quantum defect errors (0.01–0.03) typically expected for calculations of this type, based on several previous calculations in the alkaline-earth elements [3].

In Figs. 5(a)–(d) we compare experimental results with calculations that include hyperfine effects for a portion of the cross section just above the 6s threshold. Figures 5(a) and 5(b) show experiment and theory for parallel polarization, while Figs. 5(c) and 5(d) show the corresponding results for perpendicular polarization. Arrows in Figs. 5(a) and 5(c) mark the additional resonances in the calculations due to the inclusion of hyperfine effects by means of Eqs. (1)–(3). The agreement between theory and experiment here is not perfect, as discussed earlier, but it is certainly more complete since features in the cross section forbidden by the polarization-dependent selection rules are now accounted for. This small portion of the photoionization cross section was chosen to display these results (as opposed to the entire cross section in Figs. 1 and 2) because the low density of states and conspicuous forbidden lines clearly demonstrate how hyperfine effects play an important role in photoionization of barium.

A measure of the degree of hyperfine depolarization of the excited $5d6p\ ^3D_1$ state was determined by adjusting the value of $g_{\rm av}^{(2)}$ in the calculated cross section and comparing these results with the experimental measurements. In order to achieve a reliable result, we set the experimental cross section equal to the calculated cross section at the $5d_{3/2}8d$ $J=2$ resonance at 527.4 nm where theory and experiment have nearly identical line shapes. We then visually compared the height of the forbidden resonances for various values of $g_{\rm av}^{(2)}$, different from the limit of complete depolarization, $g_{\rm av}^{(2)}=0.86$. The values of $g_{\rm av}^{(2)}$ that resulted in the best overall fit for several of the forbidden lines ranged between 0.90 and 0.92. The cross sections in Figs. 5(a) and 5(c) were calculated with $g_{\rm av}^{(2)}=0.92$. A value of 0.92 indicated that the excited $5d6p\ ^3D_1$ state for the odd Ba isotopes was nearly midway between the limit of complete depolarization and the limit of no depolarization. This procedure compared a calculated absolute cross section with an experimental relative measurement which indicated the extent of depolarization of the excited state in the time-averaged sense of $g_{\rm av}^{(2)}$. For any experiment in which multimode broadbandwidth lasers with pulse durations comparable to $\omega_{FF'}^{-1}$ are used for the measurement, an attempt to determine an exact result for $g_{\rm av}^{(2)}$ from "first principles" would probably yield a meaningless result. Obtaining an indica-

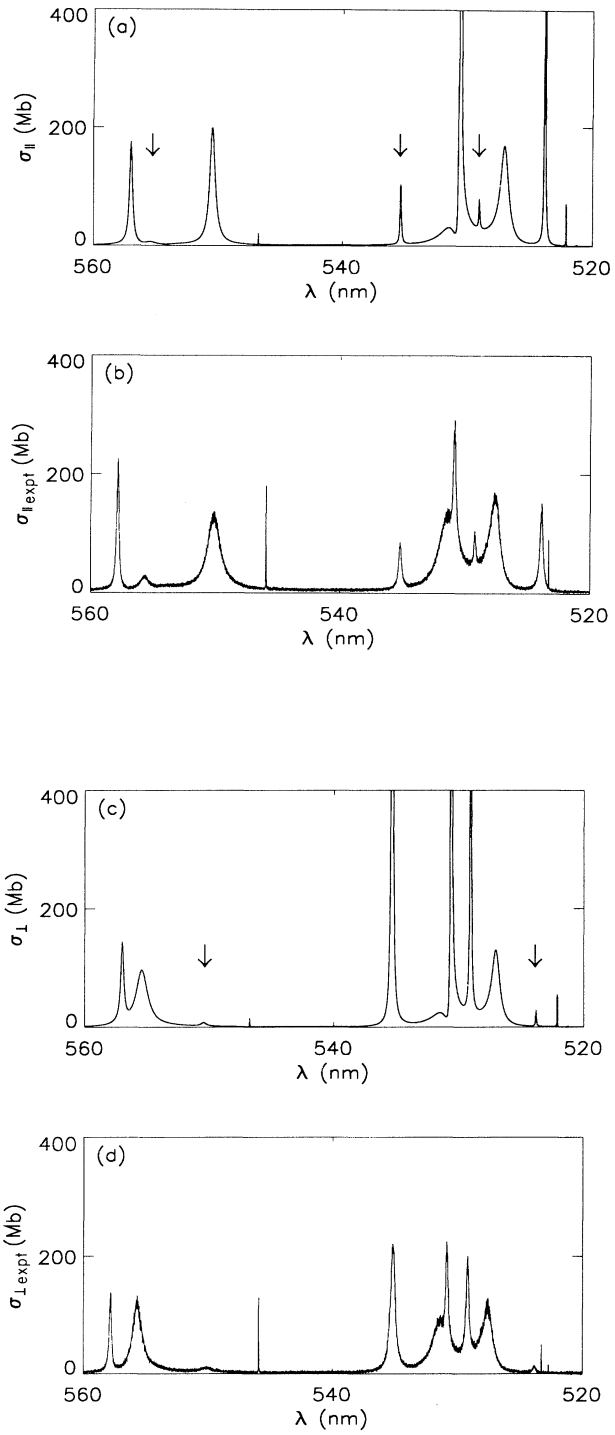

FIG. 5. (a) Calculated photoionization cross section for parallel polarization including hyperfine effects with $g_{\rm av}^{(2)}=0.92$. Arrows denote the additional (forbidden) resonances. (b) Experimental cross section for parallel polarization. (c) Calculated photoionization cross section for perpendicular polarization including hyperfine effects with $g_{\rm av}^{(2)}=0.92$. Arrows denote the additional (forbidden) resonances. (d) Experimental cross section for perpendicular polarization.

tion of the extent of depolarization was one important result of the present work. Not only did this result improve the agreement between the calculations and the experimental measurements, it provided an important consistency check on the description of hyperfine depolarization as presented in Ref. [10]. The fact that the same value of $g_{\rm av}^{(2)}$ gave the intensity of "forbidden" lines in both polarization schemes of Fig. 5 gives us additional confidence in this interpretation.

SUMMARY

We have presented both experimental and theoretical results for photoionization of the $5d6p\ ^3D_1$ state in barium for the energy range between the $6s$ threshold and 875 $\rm cm^{-1}$ above the $5d_{5/2}$ threshold. The theoretical cross sections, calculated by the eigenchannel R-matrix method in combination with MQDT methods, generally agree well with the experimental photoionization cross sections. We have shown that the addition of a simple model for the hyperfine interaction developed earlier [10] could account for forbidden features in the experimental cross sections associated with the odd isotopes of natural barium. These results further demonstrate the effectiveness of the eigenchannel R-matrix method, and emphasize the importance of the hyperfine interaction (if present and of sufficient strength) in a complete description of excited state photoionization processes. While only the $J_0=0\rightarrow J_e=1\rightarrow J_f=0$ and 2 or $J_f=1$ and 2 excitation schemes were discussed here, this work illustrates that in general selection rules on J and M_J that depend on the angle between polarization vectors can break down significantly under the influence of the hyperfine interaction.

ACKNOWLEDGMENTS

This work was supported by National Science Foundation Grant No. PHY 90-12244 to the University of Colorado. The authors thank F. Robicheaux and J. Cooper for valuable discussions, and S. J. Smith for providing technical support and the laboratory equipment necessary to complete this work.

[1] C. H. Greene and C. E. Theodosiou, Phys. Rev. A **42**, 5773 (1990).
[2] K. Bartschat and B. M. McLaughlin, J. Phys. B **23**, L439 (1990).
[3] C. H. Greene and M. Aymar, Phys. Rev. A **44**, 6271 (1991).
[4] C. E. Burkhardt, J. L. Libbert, J. Xu, J. J. Leventhal, and J. D. Kelley, Phys. Rev. A **38**, 5949 (1988).
[5] A. Kallenbach, M. Kock, and G. Zierer, Phys. Rev. A **38**, 2356 (1988).
[6] B. Willke and M. Kock, Phys. Rev. A **43**, 6433 (1991).
[7] L.-W. He, C. E. Burkhardt, M. Ciocca, J. J. Leventhal, and S. T. Manson, Phys. Rev. Lett. **67**, 2131 (1991).
[8] V. Lange, U. Eichmann, and W. Sandner, Phys. Rev. A **44**, 4737 (1991).
[9] J. S. Keller, J. E. Hunter III, and R. S. Berry, Phys. Rev. A **43**, 2270 (1991).
[10] R. P. Wood, C. H. Greene, and D. Armstrong, Phys. Rev. A **47**, 229 (1993).
[11] W. Sandner, K. A. Safinya, and T. F. Gallagher, Phys. Rev. A **24**, 1647 (1981).
[12] P. Camus, M. Dieulin, A. El Himdy, and M. Aymar, Phys. Scr. **27**, 125 (1983).
[13] M. Aymar, P. Camus, and A. El Himdy, Phys. Scr. **27**, 183 (1983).
[14] W. E. Cooke. S. A. Bhatti, and C. L. Cromer, Opt. Lett. **7**, 69 (1982).
[15] P. Grundevik, M. Gustavsson, G. Olsson, and T. Olsson, Z. Phys. A **312**, 1 (1983).
[16] M. Aymar, P. Camus, and A. El Himdy, J. Phys. B **15**, L759 (1982).
[17] M. J. Seaton, Rep. Prog. Phys. **46**, 167 (1983).